Mechanism and Modelling for Sorption of Toxic Ion on Cement Kiln Dust

A. El- Dakroury*, M.S. Sayed and E.EL- Sherif

Hot lab. Center and waste management, Atomic Energy Authority, P.O. 13759 Cairo Egypt
*eaishaw95@yahoo.com

Abstract: Cement manufacturing is a critically important industry in Egypt. The industrial by-product and waste materials must be managed responsibly to insure a clean and safe environment. Cement kiln dust (CKD) is a significant by-product material of the cement manufacturing process. Cement kiln dust is a waste residue composed chiefly of oxidized, anhydrous, micron – sized particles generated as a by product of the manufacture of Portland cement. The use of cement kiln dust as adsorbent in wastewater treatment has a great attention as cheap material and clay structure. This work will discuss the basic characteristics of CKD physical and chemical properties and regulatory requirements. The batch removal of Cr(VI) from aqueous solution using low-cost adsorbents such as cement kiln dust under different experimental conditions and the influences of initial Cr (VI) ion concentration (50 to 300 mg·l-1) and pH (1 to 4) were investigated in this study. Adsorption of Cr (VI) is highly pH-dependent and the results indicate that the optimum pH for the removal was found to be 1 for CKD. A comparison of kinetic models applied to the adsorption of Cr (VI) ions on the CKD was evaluated for the pseudo first-order, the pseudo second-order, Elovich and intraparticle diffusion kinetic models, respectively. The results showed that the pseudo second-order kinetic model was found to correlate the experimental data well.
[A. El- Dakroury, M.S. Sayed and E.EL- Sherif. **Mechanism and Modelling for Sorption of Toxic Ion on CementKiln Dust**]. Nature and Science 2011;9(5):100-108]. (ISSN: 1545-0740). http://www.sciencepub.net.

Keywords: CKD; adsorption; Cr (VI); adsorption kinetics; low-cost adsorbents.

1. Introduction:

Chromium is an important industrial metal used in various products and processes. Usually, chromium has been released to the environment via leakage, poor storage or improper disposal practices [1]. Generally, chromium in the environment is found primarily in two oxidation states: hexavalent chromium (Cr(VI)) and trivalent chromium (Cr(III)). Hexavalent chromium is relatively mobile in the environment and is acutely toxic, mutagenic, teratogenic and carcinogenic. Whilst trivalent chromium has relatively low toxicity and is immobile under moderately alkaline to slightly acidic conditions According to its toxicity, chromium was classified as a primary pollutant and ranked as second among many toxic metals in the environment [2, 3]. A number of treatment methods for the removal of metal ions from aqueous solutions have been reported as: mainly reduction, ion exchange, electrodialysis, electrochemical precipitation, evaporation, solvent extraction, reverse osmosis, chemical precipitation and adsorption.

Most of these methods suffer from drawbacks such as high capital and operational costs or the disposal of the residual metal sludge. In Egypt, production of the different types of cement reached nearly 30 million tons, with 3 millions tons CKD /year in dry lines. Up to twenty-five years ago, cement was produced by the wet process in Egypt. Nevertheless, the on-going shift in the cement industry to the dry method is expected to increase the accumulated dust. The dry process of cement production produces three

times more dust than the wet process. CKD represents a mixture of raw feed, partly calcined cement clinker, and condensed volatile salts [4-5]. The chemical composition of CKD is influenced by the size of particles carried away by the kiln gases. The released dust shows considerable amount of alkalis volatilized in the burning zone and condensed on the particles of the dust. Approximately 12% of the kiln feed exits from the kiln with the gas and about 73% of CKD is recycled to the cement making process. For example in Tourah Portland Cement Factory, the production of by-pass kiln dust per day is about 5.3% of the total production of the rotary kiln which is about 9000 ton/day. So the amount of by-pass kiln dust is about 477 ton/day Chemical coagulation, biological treatment and adsorption are the methods for the treatment of wastewater from tanneries for organic substances and heavy metals removal. The present study investigates the possibility of utilization of by-pass cement kiln dust as a adsorbent for removal of Cr (VI) from aqueous solution. A kinetic study was carried out using pH and concentration as parameters [6].

2. Experimental Procedure
Materials
Cement Kiln Dust (CKD)

Cement kiln dust (CKD) is a fine particulate material produced as a result of cement production. Cement kiln dust often consists of clinker particles,

partially calcined materials and alkali compounds, which can be high in lime content. The chemical content of CKD depends upon the raw materials, plant configuration, and the preprocessing type . Cement kiln dust as it is often used as the generic term for dust created in the kiln and collected from the cement manufacturing process. In a wet process, some of the CKD is removed from the kiln as waste dust. In a dry process, dust is collected from the kiln in precipitators. CKD removed from the clinker cooler at the end of the kiln is recalculated in the cyclone and pre-heaters (dry process). Dust collected from the upstream portion of the kiln is removed from the system as by-pass dust. The by-pass dust is removed as a precaution against materials (heavy metals, chlorides, and alkalis) that may cause the clinker to be out of specification limits.

Beneficial uses of "waste" CKD include agricultural liming agent, roadbed stabilization, and waste stabilization CKD has been used for the treatment of sand, expansive clays, and soft or wet soils .Other applications included stabilization of contaminated soil or sludge , pavement filler, and subgrade stabilization. CKD has also been used as an additive in blended cements established that CKD can used to stabilize dune sand with 12% to 50% CKD by sand weight depending upon the application. The stabilized dune sands showed higher compressive strengths with increased CKD content and increased

curing temperatures, but the samples failed in freeze-thaw durability testing. For expansive clays, CKD-clay mixture has showed to have comparable engineering properties to fly ash-soil and cement-soil mixtures. The use of CKD in stabilization of clays has showed to improve the unconfined compressive strength and reduce the plasticity index using dust with low LOI. Adding CKD with high LOI resulted in relatively lower unconfined compressive strengths and higher plasticity indices [7-10] indicated that CKD could be used as an alternative to quick lime for sub-grade stabilization in highway construction. The use of CKD as a partial cement replacement in concrete has showed to have adverse effects on strength. Using 80% cement replacement resulted in an 85% decrease in compressive strength as compared with the control. Flexural strength and modulus of rupture also decreased with increasing CKD content. Table 1. Shows the monthly change in CKD chemical composition for different batches in the Tourah Portland Cement Factory. Chemical compositions are varying from batch to batch. CaO contents range from 38% to 73%, while the silicon dioxide (SiO2) ranges from approximately 10% to 20%. The Blaine fineness, or specific surface area, of cement ranges from 300 to 500 m^2/kg as determined by ASTM C 204, Standard Test Method for Fineness of Hydraulic Cement by Air Permeability Apparatus.

Table.1: Monthly change of CKD in chemical composition

Month	Percent by Weight (%)													
	SiO^2	Al_2O_3	Fe_2O_3	CaO	MgO	SO_3	Na_2O	K_2O	TiO_2	P_2O_3	SrO	Mn_2O_3	Cl	lOI
1/06	16.46	5.63	1.69	67.11	1.56	3.37	0.39	3.62	0.25	0.08	0.06	0.02	0.00	34.68
2/06	16.80	5.60	1.56	66.96	1.56	3.39	0.58	3.77	0.24	0.09	0.05	0.02	0.00	34.98
3/06	15.86	5.54	1.79	66.99	1.66	3.79	0.30	3.66	0.24	0.09	0.05	0.03	0.00	34.97
4/06	16.18	5.79	1.66	69.27	1.66	3.30	0.18	2.29	0.26	0/09	0.06	0.02	0.00	34.35
5/06	16.72	5.70	1.95	69.63	1.58	3.14	0.21	2.14	0.26	0.10	0.05	0.02	0.00	34.00
6/06	16.78	5.60	2.03	71.50	1.58	2.51	0.16	1.78	0.25	0.09	0.07	0.02	0.00	34.09
7/06	15.16	5.15	2.07	67.85	1.41	4.05	0.23	4.06	0.23	0.09	0.06	0.02	0.00	35.99
8/06	13.76	5.00	1.92	65.77	1.39	5.38	0.30	6.23	0.21	0.09	0.06	0.02	0.00	35.17
9/06	13.86	4.98	1.96	66.46	1.34	5.32	0.27	5.91	0.23	0.10	0.05	0.02	0.00	35.41
10/06	14.32	5.11	1.98	66.57	1.40	4.52	0.25	5.34	0.23	0.10	0.05	0.02	0.00	35.41
11/06	14.03	4.96	1.93	65.17	1.37	5.19	0.62	6.65	0.22	0.09	0.04	0.02	0.00	NR
12/06	13.39	4.71	1.79	64.00	1.37	6.01	0.42	7.81	0.21	0.09	0.04	0.02	0.00	NR

Fig.1 shows the Particle Size Distribution of CKD1, CKD2, CKD3, CKD4 (batches) and OPC. The CKD1 sample was coarser than OPC on the upper end of particle sizes; between 0% and 60% passing, the CKD1sample and OPC were nearly identical. The

CKD4 sample was also coarser than cement. The gap in the distribution curve could possibly be due to dispersion during testing of the sample. The CKD3 and CKD2 samples were finer than cement. For the CKD2 sample, the coarsest 5% of particles was most

likely an artificial result of inadequate particle dispersion during the testing process. The CKD1 and CKD2 samples have otherwise similar distributions. By accounting for the lack of complete dispersion in the CKD2 sample, the maximum particle sizes are approximately 60 μm for the CKD1 and CKD2 samples. The maximum particle size for the CKD3 sample is much larger, approximately 450 μm. OPC has maximum particle sizes of around 100 μm, D of approximately 45 μm, and an average diameter of 15

μm . The D85 of the CKD1 and CKD2 samples are approximately 5 to 8 μm (including the lack of complete dispersion for the CKD1 sample).CKD1 and CKD4 samples is much larger, approximately 70 μm and 170 μm, respectively. The average diameter for the CKD1and CKD2 samples range from 4.7 to 11.9 μm (including the lack of complete dispersion for the CKD2 sample), and the CKD3 sample's average diameter is around 37 μm.
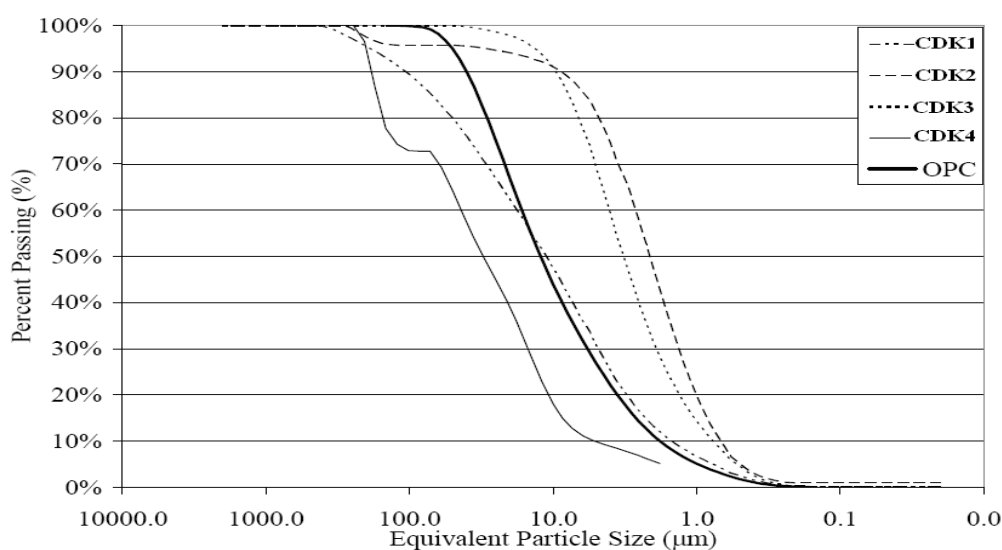

Fig. 1: Particle Size Distribution of CKD1, CKD2, CKD3, CKD4 and OPC

Table 2 indicates the specific surface area of the selected CKD. The high LOI samples (CKD1 and CKD2) were much finer than the low LOI samples,

Table   2: Specific Surface Area of OPC and different CKD

Samples	Specific Surface Area (m²/ Kg)	D(μm)	D(μm)	D(μm)	D(μm)
OPC	300-500	45	35	13	2
CKD1	3300	13	8	3	0.7
CKD2	3900	30	5	2	0.6
CKD3	1690	200	70	11	1
CKD4	230	200	170	30	5.2

Batch adsorption studies

Batch experiments with CKD1 were conducted to investigate the parametric effects of initial adsorbate concentration on Cr (VI) adsorption. Chromium samples were prepared by dissolving a known quantity of potassium dichromate ($K_2Cr_2O_7$) in double-distilled water and used as a stock solution and diluted to the required initial concentration (range: 20 to 300 mg·L-1). 50 ml of Cr(VI) solution of known concentration (Co) and initial pH was taken in a 100 ml screw-cap conical flask with a required amount of

adsorbent and was agitated at a speed of 200 rpm in a thermostatic shaker bath at 25ºC for a specified period of contact time. Then, the solution was filtered through a 0.45 μm membrane filter. The initial pH of the solution was adjusted by using either 0.1 N NaOH or 0.1 N H_2SO_4. Perkin-Elmer UV-visible spectrophotometer (model 550S) was employed with 1,5-diphenylcarbazide in acid medium to determine the remaining concentrations of Cr(VI) in the sample. The filtrate was analysed for the remaining Cr(VI) concentration. The amount of Cr(VI) adsorbed in

mg·g^{-1} at time t was computed by using the following equation:

$$q_t = \frac{(C_o - C_t)V}{m_s} \qquad (1)$$

where:

C_o, and C_t are the Cr(VI) concentrations in mg·L^{-1} initially and at a given time t, respectively

V is the volume of the Cr(VI) solutions in ml

m_s is the weight of activated carbon in g.

The percentage of removed Cr(VI) ions (R_{em} %) in solution was calculated using Eq.(2):

$$R_{em}\,(\%) = \frac{(C_o - C_t)}{C_o} x100 \qquad (2)$$

The effect of initial concentration of Cr(VI), contact time and initial pH were investigated by varying any one of the process parameters and keeping the other parameters constant. Adsorption dynamics describes the solute uptake rate and evidently this rate controls the residence time of adsorbate uptake at the solid-solution interface. The kinetics of Cr(VI) adsorption on the CKD were analysed using pseudo first-order [11] pseudo second-order [12], Elovich [13,14] and intraparticle diffusion kinetic models. The conformity between experimental data and the modelpredicted values was expressed by the correlation coefficients (r^2, values close or equal to 1). A relatively high r^2 value indicates that the model successfully describes the kinetics of Cr(VI) adsorption. The pseudo first-order equation [11] is generally expressed as follows:

The pseudo first-order equation

$$\frac{dq_t}{dt} = k_1(q_e - q_t) \qquad (3)$$

where:

q_e and q_t are the adsorption capacity at equilibrium and at time

t, respectively (mg·g-1),

k_1 is the rate constant of pseudo first-order adsorption (l·min^{-1}).

After integration and applying boundary conditions t = 0 to t = t and

q_t = 0 to q_t = qt, the integrated form of Eq. (3) becomes:

$$log(q_e - q_t) = log(q_e) - \frac{k_1}{2.303}t \qquad (4)$$

The values of log (qe - qt) were linearly correlated with t. The plot of log (q$_e$ - q$_t$) vs. t should give a linear relationship from which k_1 and q_e can be determined from the slope and intercept of the plot, respectively.

The pseudo second-order equation

The pseudo second-order adsorption kinetic rate

equation [12]

$$\frac{dq_t}{dt} = k_2(q_e - q_t)^2 \qquad (5)$$

where:

k_2 is the rate constant of pseudo second-order adsorption (g·mg-1·min^{-1}). For the boundary conditions t = 0 to t = t and q_t = 0 to q_t = q$_t$, the integrated form of Eq. (5) becomes:

$$\frac{1}{(q_e - q_t)} = \frac{1}{q_e} + k\,t \qquad (6)$$

which is the integrated rate law for a pseudo second-order reaction. Equation (6) can be rearranged to obtain Eq.(7), which has a linear form:

$$\left(\frac{t}{q_t}\right) = \frac{1}{k_2\,q_e^2} + \frac{1}{q_e}(t) \qquad (7)$$

if the initial adsorption rate, h (mg·g-1·min-1) is:

$$h = k_2\,q_e^2$$

Then Eqs. (7) and (8) become:

$$\left(\frac{t}{q_t}\right) = \frac{1}{h} + \frac{1}{q_e}(t) \qquad (9)$$

The plot of (t/qt) and t of Eq. (7) should give a linear relationship from which q$_e$ and k_2 can be determined from the slope and intercept of the plot, respectively.

The Elovich equation

The Elovich model equation is generally [13, 14]

$$\frac{dq_t}{dt} = \alpha\,exp\left(-\,\beta\,q_t\right)$$

where:

α is the initial adsorption rate (mg·g-1·min-1)

β is the desorption constant (g·mg-1) during any one experiment

To simplify the Elovich equation, [17] assumed α βt >> t and by applying the boundary conditions qt = 0 at t = 0 and qt = qt at t = t Eq.(10) becomes:

$$q_t = \frac{1}{\beta}\,ln(\alpha\,\beta) + \frac{1}{\beta}ln(t) \qquad (11)$$

If Cr(VI) adsorption fits the Elovich model, a plot of qt vs. ln (t) should yield a linear relationship with a slope of (1/β) and an intercept of (1/β) ln(αβ).

The intraparticle diffusion model

The intraparticle diffusion model is expressed as [18, 19]

$$R = k_{id}(t)^a \qquad (12)$$

A linearised form of the equation is followed by

$$logR = logk_{id} + a\,log(t)$$

where:

R is the per cent Cr(VI) adsorbed

t is the contact time (h)

a is the gradient of linear plots

k_{id} is the intraparticle diffusion rate constant (h-1) a depicts the adsorption mechanism

k_{id} may be taken as a rate factor, i.e., per cent Cr(VI) adsorbed per unit time.

The values of k_{id} were calculated from the slope of such plots (plots not shown here) and the r^2 values led to the conclusion that the intraparticle diffusion process is the rate-limiting step. Higher values of k_{id} illustrate an enhancement in the rate of adsorption, whereas larger kid values illustrate a better adsorption mechanism, which is related to an improved bonding between Cr(VI) ions and the adsorbent particles .

3. Results and Discussion
Effect of pH

The removal of Cr(VI) by three types of CDK (CDK1, CDK2 and CDK3) at different pHs at an initial Cr(VI) concentration of 100 mg·l-1, a temperature of 25ºC, particle size of 1.00 to 1.25 mm and agitation speed of 200 r·min-1 are shown in Figs. 2 to 4. The adsorption of Cr(VI) occurred in two stages. The first stage was solute uptake i.e. the immediate solute uptake achieved within a few hours, followed by the second stage, i.e. the subsequent uptake of solute, which continued for a long time period. For CKD2, the amount adsorbed increased from 4.21 to 20.98 mg·g-1 as the pH decreased from 4 to 1. While for CKD3, the amount adsorbed increased from 11.44 to 20.98 mg·g-1 as the pH decreased from 4 to 1. For CKD4, the amount adsorbed increased from 14 to19.98 mg·g-1 as the pH decreased from 4 to 1. The variation in adsorption capacity in this pH range is largely due to the influence of pH on the adsorption characteristics of the carbon which indicates that the adsorption capacity of the adsorbent is clearly pH dependent. The optimum pH was observed with 99.9 % Cr(VI) removal at pH 1.0. Chromium exists mostly in two oxidation states which are Cr(VI) and Cr(III) and the stability of these forms is dependent on the pH of the system . It is well known that the dominant form of Cr(VI) at pH 2 is $HCrO_4^-$ Increasing the pH will shift the concentration of $HCrO_4^-$ to other forms, CrO_4^{2-} and $Cr_2O_7^{2-}$. Maximum adsorption at pH 1.0 indicates that it is the $HCrO_4^-$ form of Cr(VI), which is the predominant species between pH 1 and 4, which is adsorbed preferentially on the adsorbents. Results also show that the adsorption reaction can be approximated with the pseudo second-order kinetic model. The smallest value of correlation coefficient was > 0.991 (Table 3). The rate constants are represented in Table 2. It can be observed that h is generally higher for CDK4 than that of CDK2 and CKD3

Effect of initial chromium ion concentrations

The removal of Cr(VI) by adsorption on different CKD were shows to increase with time and attained a maximum value at 72 h, and thereafter, it remained almost constant. On changing the initial concentration of Cr(VI) solution from 20 to 300 mg·L-1, the amount adsorbed increased from 10.60 mg·g-L (99.99 % removal) to 59.40 mg·g-L (99.0 % removal) at 25 ºC, pH 1.0 from Figs. 5 a, b and c the results indicate that the amount of adsorbate on the solid phase with lower initial concentration of adsorbate was smaller than the amount when higher initial concentrations were used. It was clear that the removal of Cr(VI) was dependent on the concentration of Cr(VI) because the decrease in the initial Cr(VI) concentration increased the amount of Cr(VI) adsorbed. .

The experimental points shown together with the theoretically generated curves Fig. 5 a, b and c reflect the extremely high correlation coefficients shown in Table 4. The data showed good compliance with the pseudo second-order kinetic model ($r^2 > 0.989$). The values of the rate constants, k_2, were found to increase from 48.10-5 to 58.10-3 (l·mg-L·min-1) with decrease in the initial Cr(VI) ion concentration from 300 to 20 mg·L/l.

The rate constants are represented in Table 3 It can be observed that h is generally higher for CDK4 than that of CKD2 and CKD3
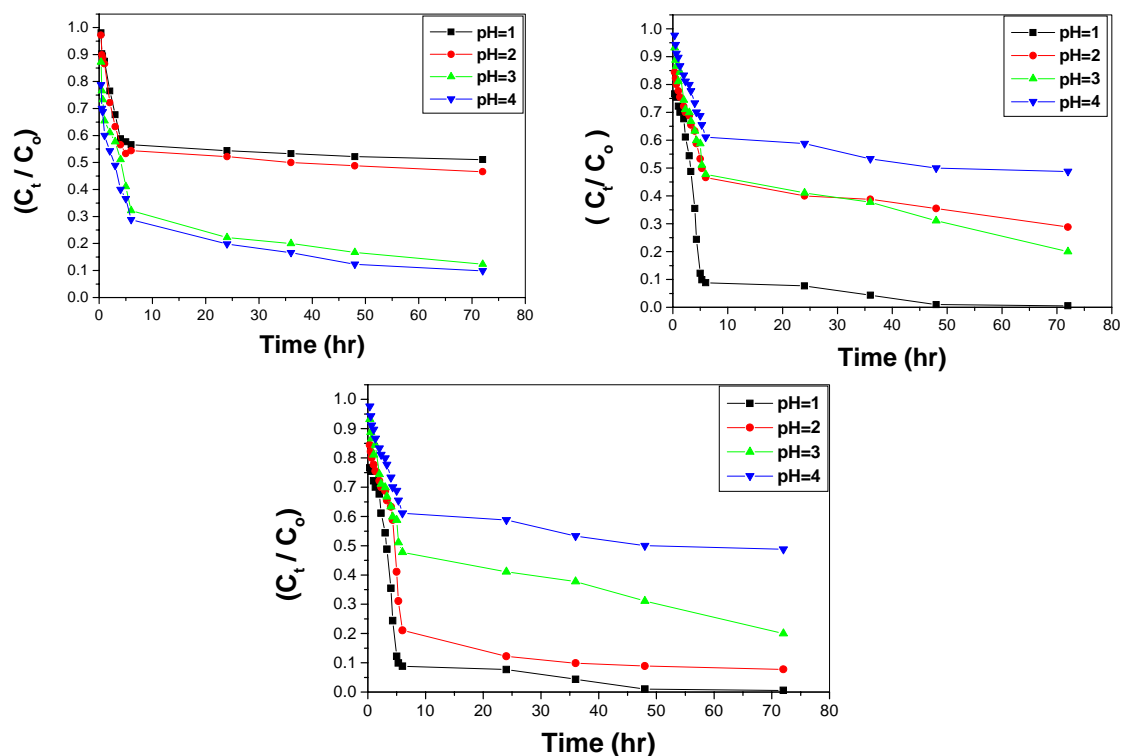
Fig. 2 a, b and c: Time variations of Cr (VI) adsorption on CKD1, CKD2 and CKD3 at different pHs

Table   3: Adsorption kinetic model rate constant for the different CKD at different pHs

Adsorbent	Initial pH	Pseudo first – order		Pseudo second – order			Elovich model			Intraparticle diffusion		
		k_1	r^2	k_2	h	r^2	β	α	r^2	k_{id}	a	R^2
CKD1	1.0	0.226	0.978	0.0091	10.891	0.898	32991	0.131	0.889	29.328	0.422	0.900
	2.0	0.108	0.892	0.0037	6.608	0.986	16704	0.139	0.974	18.934	0.488	0.981
	3.0	0.035	0.898	0.031	1.566	0.983	2421	0.241	0.977	4.633	0.600	0.970
	4.0	0.182	0.8325	0.053	1.066	0.899	4.00	0.643	0.988	2.086	1.008	0.98
CKD2	1.0	0.113	0.977	0.022	27.123	0.988	213.91	0.107	0.982	60.511	0.160	0.963
	2.0	0.106	0.973	0.015	16.503	0.98	75.13	0.188	0.965	41.537	0.300	0.986
	3.0	0.1733	0.966	0.029	12.080	0.988	112.70	0.243	0.948	32.943	0.1.71	0.897
	4.0	0.131	0.966	0.012	4.583	0.989	17.057	0.343	0.977	13647	0.435	0.899
CKD3	1.0	0.087	0.977	0.00122	0.963	0.996	33.923	47.988	0.481	33.676	0.311	0.987
	2.0	0.094	0.887	0.0033	0.881	0.989	16.705	9.876	0.765	16.987	0.499	0.943
	3.0	0.029	0.986	0.027	0.865	0.999	2.341	9.654	0.453	14.987	0.572	0.954
	4.0	0.0498	0.765	0.034	0.765	0.989	3.885	8.6732	0.436	11.997	1.008	0.989

Table4 (a) adsorption kinetic model rate constant for the CKD1 at different initial chromium ion concentrations

C_o(mg/l)	Pseude first – order		Pseude second – order			Elovich model			Intraparticle diffusion		
	k_1	r^2	k_2	h	r^2	β	α	r^2	k_{id}	a	R^2
50	0.324	0.963	0.0591	17.999	0.984	410.537	0.389	0.987	57.200	0.178	0.917
100	0.199	0.989	0.0072	11.771	0.987	33.993	0.122	0.899	37.100	0.411	0.898
200	0.090	0.887	0.0008	9.733	0.898	11.995	0.065	0.875	8.521	0.711	0.984
300	0.078	0.987	0.0007	4.321	0.899	23.011	0.032	0.876	7.3241	0.701	0.985

Table5 adsorption kinetic model rate constant for the CKD2 at different initial chromium ion concentrations

C_o(mg/l)	Pseude first – order		Pseude second – order			Elovich model			Intraparticle diffusion		
	k_1	r^2	k_2	h	r^2	β	α	r^2	k_{id}	a	R^2
50	0.312	0.897	0.0574	19.111	0.896	412.500	0.467	0.984	57.200	0.188	0.887
100	0.199	0.890	0.0091	12.681	0.893	32.971	0.134	0.897	35.180	0.366	0.890
200	0.085	0.972	0.0008	9.764	0.821	13.444	0.067	0.945	8.521	0.732	0.897
300	0.066	0.876	0.0004	5.022	0.889	23.011	0.064	0.987	7.4321	0.537	0.879

Table6 adsorption kinetic model rate constant for the CKD3 at different initial chromium ion concentrations

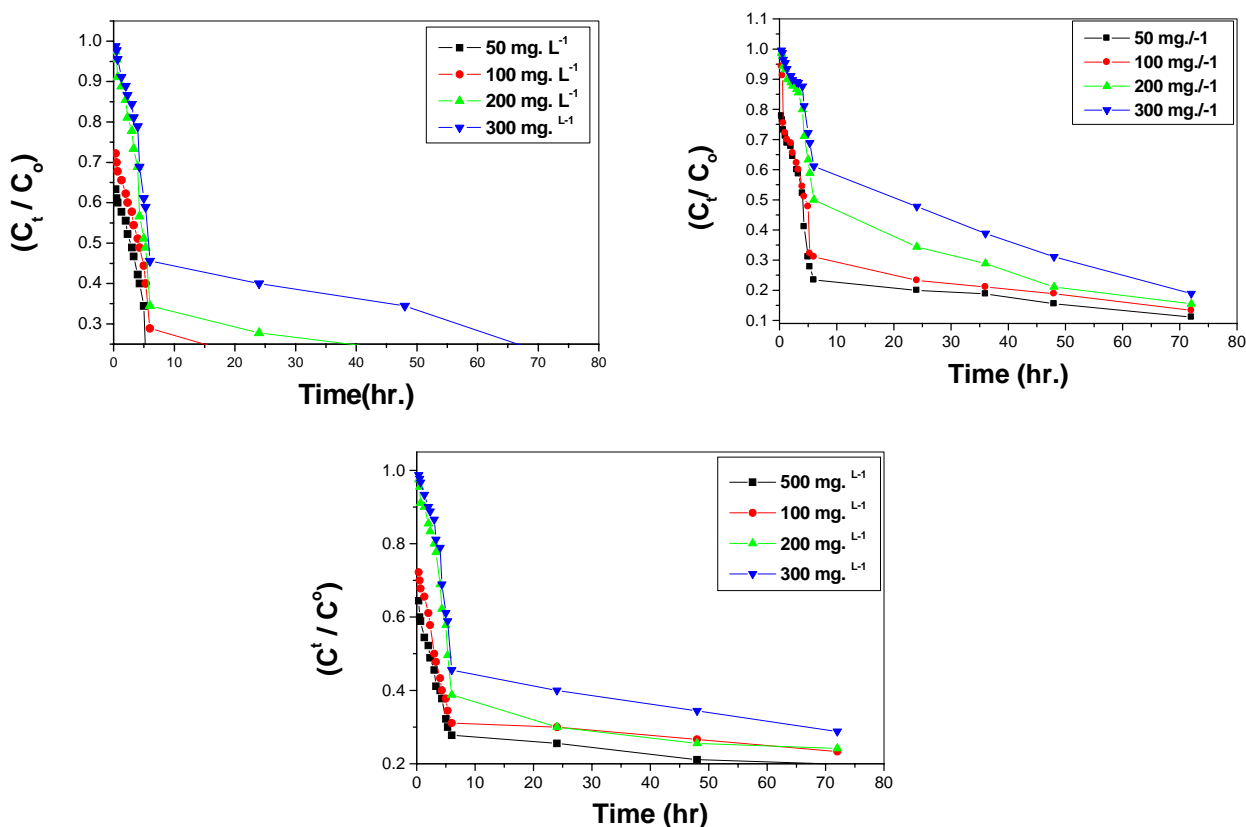| C_o(mg/l)	Pseude first – order		Pseude second – order			Elovich model			Intraparticle diffusion		
	k_1	r^2	k_2	h	r^2	β	α	r^2	k_{id}	a	R^2
50	0.200	0.888	0.0632	19.029	0.976	408.511	0.501	0.991	57.876	0.196	0.875
100	0.211	0.899	0.0512	11.893	0.899	34.007	0.156	0.897	37.063	0.401	0.900
200	0.092	0.867	0.0005	8.896	0.986	14.006	0.049	0.976	10.122	0.681	0.970
300	0.076	0.923	0.00033	5.0112	0.889	23.001	0.044	0.976	8.0211	0.743	0.986

Fig. 3 a, b and c: Time variations of Cr(VI) adsorption on CKD1, CKD2 and CKD3 at different concentrations

4. Conclusion
    The volume of by-product materials generated

from core-sector industries such as cement, power, steel, and other mining and heavy industries are

increasing. The cost of disposal is continuing to grow day-by-day in our society. The growth of by-product materials is inevitable unless new and beneficial use options, which are economically sound and environmentally friendly, are developed and implemented. Cement kiln dust (CKD) is a by-product material of cement manufacturing industry. It is a fine powdery material similar in appearance to Portland cement. The principal constituents of CKD are compounds of lime, silica, and alumina, and iron.

The physical and chemical characteristics of CKD depend on the raw materials used and the method of its collection employed at a particular cement plant. Free lime is found in CKD. The concentration of free lime is generally highest in the coarser particles of CKD captured closest to the kiln. Finer particles of CKD contain higher concentrations of sulfates and alkalis. The primary value of cement kiln dust is its cementitious property. Depending on the concentration of lime (CaO), CKD can be highly cementitious

Our results indicate that cement kiln dust could be recommended as a material for the effective removal of metal pollutants from industrial wastewaters. The results of this study have shown that CKD (a cheap by-product of cement industry) is efficient in the processes of removal of Cr (VI) from aqueous solution. CKD was the most effective, for which the removal reached 99.99 % Cr (VI) at 25ºC. Adsorption of Cr (VI) was highly pH-dependent and the results showed that the optimum pH for the removal was found to be 1, at which Cr (VI) exists mostly as the most easily adsorbed form, $HCrO_4^-$ increases as the initial Cr(VI) concentration and contact time were found to increase the percentage removal of Cr(VI). The kinetics of the Cr(VI) adsorption on the different adsorbents was found to follow a pseudo second-order rate equation.

Corresponding author
A. El- Dakroury
Hot lab. Center and waste management, Atomic Energy Authority, P.O. 13759 Cairo Egypt
eaishaw95@yahoo.com

5. References:
1- Suwannee Junyapoon and Suttawadee Weerapong (2006) "Removal of hexavalent chromium from aqueous solution by scrap iron filings kmitl " Sci. Tech. J. Vol. 6 No. 1 2- Kim Y. Kim J.H. , Lee K.G. and Kang S.G(2005)" Adsorption behavior of heavy metal ions in the solutions of clay minerals under various conditions" Journal of Ceramic Processing Research. Vol. 6, No. 1, pp. 25~30

3- 4-Kobya M, (2004) "Adsorption, kinetic and equilibrium studies of Cr(VI) by hazelnut shell activated carbon". Adsorb. Sci. Technol. 22 51-64.

4- Heechan Cho, Dalyoung Ohand and Kwanho Kim (2005) "A study on removal characteristics of heavy metals from aqueous solution by fly ash", J. Hazard. Material   127 187–195.

5-Katz, A., and Kovler, K., (2004) "Utilization of industrial by-products for the roduction, of controlled low-strength materials (CLSM)," Waste Management, V. 24, No. 5, pp. 501-512.

6- Wayne S. Adaska, P.E., 2008 , "Beneficial uses of cement kiln dust" Presented IEEE/PCA 50th Cement Industry Technical Conf., Miami, FL,

7- Badmus M.A.O. , Audu T.O.K. and Anyata B.U. (2007) "Removal of heavy metal from industrial wastewater using hydrogen peroxide, African Journal of Biotechnology" Vol. 6 (3), pp. 238-242,

8- Miller, G.A., and Zaman, M., (2000) "Field and laboratory evaluation of cement kiln dust as a soil stabilizer," Transportation Research Board, Washington, D.C., No. 1714, pp. 25-32.

9- Shoaib, M.M., Balaha, M.M., and Abdel-Rahman, A.G., (2000) "Influence of cement kiln dust substitution on the mechanical properties of concrete," Cement and Concrete Research, V. 30, pp. 371-377

10- IEEE-IAS Cement Industry Committee (2008) "Beneficial uses of cement kiln dust presented at IEEE/PCA 50th Cement Industry Technical Conf., Miami, FL, 19-22, 1.

11- Zhu, J-H., Zaman, M., and Laguros, J.G., (1999) "Resilient modulus and microstructure of cement kiln dust stabilized base/subbase aggregate," Soils and Foundations, Japanese Geotechnical Society, V. 39, No. 6, pp. 33-42.

12- Lagergren S   (1898) Zur theorie der sogenannten adsorption geloster stoffe. Kungliga Svenska Vetenskapsakademiens. Handlingar 24 1-39.

13- HO YS, McKAY G, Wase Daj and Foster CF (2000) Study of the sorption of divalent metal ions on to peat. Adsorp. Sci. Technol. 18 639-650.

14- Chien sh and   Clayton (1980) Application of elovich equation to the kinetics of phosphate release and sorption on soils. Soil Sci. Soc. Am. J. 44 265-268.

15- Sparks dl (1986) Kinetics of Reaction in Pure and Mixed Systems, in Soil Physical Chemistry. CRC Press, Boca Raton.

16- Weber WJ and Morris JC (1963) Kinetics of adsorption on carbon from solution. J. Sanit. Eng. Div. Am. Soc. Civ. Eng. 89 31-60.

17- Deborah N. Huntzinger, Thomas and Eatmon D. (2008) "A life-cycle assessment of portland cement manufacturing: comparing the traditional process with alternative technologies Journal of Cleaner Production 1–8

18- Donghee Park, Yeoung-Sang Yun, , Dae Sung Lee, Seong-Rin Limc and Jong Moon Park (2006) "Column study on Cr(VI)-reduction using the brown seaweed " Journal of Hazardous Materials B137 1377–1384

19- Ahmad Nik, Nizam Malek Nik and Alias Mohd Yusof "Removal of Cr (III) from aqueous solutions using zeolite NaY prepared from rich husk ash" (2007) The alaysian Journal of Analytical Sciences, Vol. 11, No 1 76-8376

3/25/2011